CONSTRAINING THE GREENLAND FIRN AQUIFER'S ABILITY TO HYDROFRACTURE A CREVASSE TO THE BED OF THE ICE SHEET

by

Laura McNerney

A thesis submitted to the faculty of
The University of Utah
in partial fulfillment of the requirements for the degree of

Master of Science

Department of Geography

The University of Utah

May 2016

The University of Utah Graduate School

STATEMENT OF THESIS APPROVAL

The thesis of **Laura McNerney**

has been approved by the following supervisory committee members:

Richard R. Forster	, Chair	**1/22/16** Date Approved
Marc Calaf	, Member	**1/22/16** Date Approved
Kathleen Nicoll	, Member	**1/22/16** Date Approved

and by **Andrea R. Brunelle**, Chair/Dean of

the Department/College/School of **Geography**

and by David B. Kieda, Dean of The Graduate School.

ABSTRACT

Spanning 1.7 million km^2 with glacial ice that exceeds 3,000 m thick in the interior, the Greenland ice sheet plays a large role in Earth's response to climate change. A recently discovered firn aquifer within the ice sheet has the potential to buffer or enhance sea level rise by retaining or outputting its contents into the ocean. This study examines englacial hydrology to determine if the subsurface firn aquifer can discharge water into the ocean via hydraulic fracturing of crevasses. National Aeronautics and Space Administration (NASA) Operation Ice Bridge Accumulation Radar and Airborne Topographic Mapper data is used to map the top of the aquifer and ice surface elevation profiles by measuring water-table return signals. These profiles are input into a groundwater flow model (SEEP2D), based on Darcy's law, to determine the aquifer's potential water discharge into an existing crevasse at the lower elevation end of the aquifer profile. Next, conservation of mass equations are implemented to yield water depths in the crevasse at varying crevasse dimensions. This water depth is converted into pressure and compared with known fracture thresholds to determine the likelihood of ice failure at the base of the crevasse using the various initial crevasse dimensions. Model simulations show that the aquifer can provide enough water to propagate fracture, for 30 m deep or greater crevasses, to the base of the ice sheet within a few weeks during the melt season (when it is assumed water can discharge from the aquifer into an open crevasse). This implies the aquifer has the potential to route water to the bed of the ice

sheet where it can effect outlet glacier flow velocity and provide a direct conduit for water discharge from the inland aquifer to the global ocean.

TABLE OF CONTENTS

LIST OF FIGURES

Figures

ACKNOWLEDGEMENTS

I would like to express my appreciation to Professor Richard Forster for his patient guidance and constructive criticism. I am also thankful for Professor Kip Solomon's valuable insight into groundwater dynamics, thereby allowing me to explore applications to an ice sheet. A big thanks to Professor Kathleen Nicoll for her advice and assistance in keeping my progress on schedule. Assistance and technical guidance provided by Clément Miège, Olivia Miller, and Professor Marc Calaf is greatly appreciated. My completion of this project could not have been accomplished without the ever helpful office staff, MaryAnn Golightly, Lisa Clayton, and Pam Mitchell. Finally, I would like to thank Nicolas Bertagnolli for his steady support and my parents for their constant encouragement and confidence.

CHAPTER 1

INTRODUCTION

The Greenland ice sheet spans 1.7 million km^2 [*Bamber et al.,* 2001] with glacial ice that exceeds 3,000 m thick in the interior. This ice sheet plays a large role in the Earth's response to climate change and contains the second largest ice volume, next to the Antarctic ice sheet. Greenland's ice mass has the potential to raise sea level by seven meters, which could alter ocean and atmospheric circulation patterns [*Stocker*, 2013]. Mass loss from the Greenland ice sheet has been accelerating in the past few decades [*Shepherd et al.,* 2012; *Zwally et al.,* 2002], thus contributing to global sea level rise.

Sea level has been rising on average 3.2 mm per year since 1993 and is expected to increase exponentially as temperatures increase globally [*Stocker*, 2013]. Since the oceans span approximately 360 million km^2, a 3.2 mm increase equates to 1,152 billion m^3 of new water input into the oceans annually. Increasing volumes of water are disrupting ecosystems and burdening low lying countries [*Stocker*, 2013]. Elevated ocean levels cause coastal communities to become more stressed, as coastlines erode and groundwater wells become saline due to saltwater intrusion. The amount of new water contributing to sea level rise (as opposed to thermal expansion of existing ocean water) is dominated by the mass loss from the Greenland and Antarctic ice sheets. The Greenland ice sheet absorbs and stores a considerable amount of water in saturated pore spaces and

subsurface cavities before runoff proceeds into the ocean [*Harper et al.,* 2012]. Meltwater runoff accounts for half of Greenland's mass loss [*van den Broeke et al.,* 2009], and how this melt water reaches the ocean is poorly understood. Warming temperatures have increased surface melt and simultaneously increased ice transfer to low elevations. Crevasse extent has expanded, due to the warming, which enhances propagation of meltwater to the base of the ice sheet [*Colgan et al.,* 2011]. This is largely responsible for the increase of surface to bed drainage events that have recently been observed on timescales of days [*Boon and Sharp,* 2003] and even hours [*Das et al.,* 2008]. A recently discovered subsurface firn (partially compacted snow and ice) aquifer located in southeast Greenland persists during the winter and has potential to buffer or enhance global sea level rise [*Forster et al.,* 2013]. This study, therefore, explores one option of how water from the subsurface firn aquifer might exit the Greenland ice sheet, by analyzing crevasses as a mechanism for routing water to the bed of the ice sheet.

This study investigates the possibility of the Greenland firn aquifer behaving like a terrestrial groundwater transport system by delivering water to an open crevasse at the aquifer's lower elevation termination and by hydrologic fracturing of crevasses to the base of the ice sheet as a mechanism for water exiting the aquifer. This study attempts to answer the following questions by coupling a groundwater flow model and a hydrofracture model.

1. How much water is flowing through the Greenland aquifer along a flowline feeding Helheim Glacier?
2. Is there enough water flowing from the aquifer along this flowline, discharging into a crevasse, to yield adequate pressure within the crevasse and thus propagate

a fracture to the ice sheet bed?

If the answer to the second question is yes, then there is a direct self-propagating path for water to reach the ocean, contribute to sea level rise, and influence outlet glacier ice dynamics by reducing bed friction.

CHAPTER 2

LITERATURE REVIEW

This section reviews the hydrology of the Greenland ice sheet and explains how research has evolved into understanding fracture mechanics and the Greenland aquifer. This literature review begins with background on water transport and storage across the ice sheet and transitions into current research on the aquifer and fracture mechanics. Previous research accomplishments will be explained to highlight how the project builds on past knowledge to increase awareness of glacial hydrology and to better understand sea level rise.

2.1 Greenland Hydrology

The movement of water through the Greenland ice sheet is required for understanding how sea level will rise in the coming century. The mass balance of the Greenland ice sheet is the culmination of melt water runoff, precipitation minus iceberg calving, evaporation, and ice sublimation [*Rennermalm et al.,* 2013]. The accumulation zone is the region on the ice sheet where snowfall exceeds runoff, and the ablation zone defines regions where a combination of melt, sublimation, and calving exceed precipitation. These zones are separated by the equilibrium line altitude.

Glacial melt water travels to the ocean through a variety of transport mechanisms.

Water may be transported supraglacially via stream networks on top of the ice sheet. This surface water on the ice sheet can then be drained in the ablation zone where lakes and rivers transport water to the base of the glacier via crevasses and moulins. When crevasses contain enough water, these fractures in the ice deepen to route water into the ice sheet [*Cuffey and Paterson,* 2010]. This increases ice surface velocity five to ten times, due to the fracture opening [*Doyle et al.,* 2013]. Moulins, near vertical shafts where water propagates downwards within the ice [*Fountain and Walder,* 1998], also deliver water to the base of the glacier [*Catania,* 2008]. This water is routed through channels at the glacier bed, but many uncertainties exist about these drainage systems [*Rennermalm et al.,* 2013]. The accepted model is Röthlisberger's R-channel theory that employs the following conservation principles [*Röthlisberger,* 1972]. Conservation of energy is used to explain how energy is transformed. Thermal energy is absorbed by water and by melting ice tunnels, while thermal energy is generated due to the frictional movement of water against the ice. This energy forms the basis of how conduits melt to allow water flow through the ice sheet. Conservation of mass is always applied in such a way that water is conserved, whether it melts or refreezes, as it flows through the glacier [*Walder,* 2010]. These channels and fractures within the ice make up the network of water pathways through the glacier and allow water to exit the ice sheet at the margins.

Water may also be stored in and on the ice sheet for a period of time before being routed to the base of the glacier. Glaciers are commonly thought to delay runoff and provide water storage by holding precipitation in the form of ice, snow, or water [*Jansson,* 2003]. This water reserve is dependent on climatic factors and stores a majority of the world's fresh water. Water may be retained in the pore spaces of the glacier and

form an underground aquifer or refreeze as the water percolates through the ice [*Pfeffer et al.,* 1991]. Instead of pooling inside the ice sheet, water may be temporarily stored in supraglacial lakes. These lakes form in topographic depressions on top of the ice and increase ablation by lowering surface albedo [*Tedesco and Steiner,* 2011]. The lakes cover extensive areas, most notably in southwest Greenland, and can empty and refill rapidly during warm summer months [e.g., *Das et al.,* 2008]. These large scale drainage events periodically propagate meltwater to the bed [*Zwally et al.,* 2011] and can cause outburst floods to the detriment of towns and cities near glacially-fed rivers. On the Greenland ice sheet, drainage to the bed causes basal sliding of outlet glaciers that can result in accelerated mass ice discharge into the oceans, by lubricating the base of the ice and reducing friction between the bed and the glacier [*Lampkin et al.,* 2013; *Tedesco et al.,* 2013; *van de Wal,* 2008*; Jansson,* 1995]. Basal sliding is also enhanced from increased pressure on the ice at the bed, due to water addition. As ice discharge increases, the surface of the glacier is exposed at lower elevations [*Cuffey and Paterson,* 2010]. Warmer temperatures at these lower elevations further melt the ice, contribute to this positive feedback mechanism, and have potential to accelerate sea level rise contributions from areas of the ice sheet drained by outlet glaciers where surface water is delivered to the bed.

Recent advances in satellite measurements have allowed more precise surface mass balance measurements. For instance, measurements from the Gravity Recovery and Climate Experiment (GRACE) satellite have shown that the Greenland ice sheet experienced an average of 240 ± 18 Gt per year of ice mass loss between 2002 and 2011 [*Sasgen et al.,* 2012]. Since the 1960s, mass loss on the Greenland ice sheet has nearly

tripled [*Shepherd et al.,* 2012], due to the fact that increasing accumulation within the ice sheet has been exceeded by calving and melt [*Zwally et al.,* 2011]. More water is being stored in and routed through the glaciers via englacial conduits, calving, or subglacial aquifers due to ice sheet melt in a warming climate [*Stocker,* 2013].

2.2 Internal Accumulation

Meltwater accumulates within the Greenland ice sheet in a frozen state via two different processes. The first process occurs from meltwater that refreezes once it percolates into the cold firn and the second occurs when the water held by capillary forces freezes [*Schneider and Jansson,* 2004]. Water can freeze and thaw numerous times before being released from the ice sheet, which makes estimating firn runoff challenging. As temperatures warm, it is predicted that the firn layer will disappear [*De Woul,* 2006], which would reduce water retention within the ice sheet and amplify peak discharge [*Braun et al.,* 2000]. Secondly, the capillary component of water accumulation in the ice sheet is calculated from firn porosity and residual water content [*Schneider and Jansson,* 2004]. The firn porosity is the ratio of pore volume to total volume, and the residual water content is the water retained in the pores that cannot be released due to gravity. Widespread Greenland mass loss [*Hanna et al.,* 2008] suggests that melt loss by firn storage may become increasingly important as more melt occurs within the percolation zone [*Rennermalm et al.,* 2013]. More attention should be given to internal accumulation as the climate continues to warm and questions arise such as will the ice sheet retain melt water or will water quickly run off into the ocean?

A firn aquifer was recently discovered in southeast Greenland and is estimated to

encompass 70,000 km^2 [*Forster et al.,* 2013], with the potential to output 140 ± 20 Gt of water into the ocean [*Koenig et al.,* 2014]. This suggests that the ice sheet is currently retaining melt water, since an aquifer is a geological formation that stores water within a porous medium below the surface. For the Greenland firn aquifer, water is stored between the particles of ice, which has the potential to buffer or enhance sea level rise by retaining or outputting water. Two aquifers, a firn mountain glacier aquifer, and a groundwater aquifer are compared with the Greenland aquifer to better understand Greenland's characteristics. The difference between a confined groundwater aquifer and a firn mountain glacier aquifer is that the spatial extent of the mountain firn aquifer continually changes and water exists only seasonally, whereas for confined groundwater aquifers the spatial extent is fixed and water persists annually [*Kawashima et al.,* 1993]. Fountain [1989] considers the mountain glacier firn aquifer to be a perched unconfined aquifer that employs crevasses to drain into otherwise impenetrable ice. The Greenland aquifer is considered to act similarly to a mountain glacier firn aquifer in that its spatial extend is variable. The Greenland aquifer, however, acts more like a confined groundwater aquifer, in that water persists annually in the Greenland aquifer, while water exists only seasonally in temperate glacier firn aquifers. The Greenland aquifer persists through the winter due to extensive summer surface melt stored within large subsurface pore spaces, followed by high snowfall amounts beginning in early autumn providing thermal insulation of the melt water [*Munneke et al.,* 2014]. This aquifer in Greenland is thus able to store heat and water at depth through the winter [*Miège et al.,* 2015]. For a mountain glacier firn aquifer, water input varies daily and seasonally, and the aquifer water depth is predominantly controlled by crevasse spacing [*Fountain and Walder,*

1998]. The velocity of water flow through the firn is highly variable, as crevasses vary in spacing and depth. While the Greenland firn aquifer exhibits similar properties to groundwater aquifers and mountain glacier aquifers, there are distinct differences that must be taken into account.

Research suggests that storing surface water within the firn will delay contributions to sea level rise and eventually numerous infiltration events will completely fill the pore spaces with water [*Harper et al.,* 2012; *Schneider and Jansson,* 2004]. In recent decades, firn pore space is filling more rapidly with water and the percolation zone is spreading into previously dry snow regions [*Harper et al.,* 2012]. This has significance because the regeneration of the dry firn column takes extensive time and must be conducted in small increments. It is therefore crucial to understand the movement of water through the ice sheet to estimate the effects of climate change and implications for sea level rise. Water movement is directly dependent on hydraulic conductivity, and a study was conducted to measure the hydraulic conductivity of water through a firn aquifer within a mountain glacier, revealing the hydraulic conductivity to equal 1×10^{-5} m/s by using two pumping tests during the ablation season [*Oerter and Moser*, 1982]. Our team conducted field measurements in April 2015 on the Greenland ice sheet near Helheim Glacier revealing hydraulic conductivity values of 1.88×10^{-4} m/s. Hydraulic conductivity measurements can vary over many orders of magnitude in a single terrestrial groundwater system [*Schwartz and Zhang*, 2003]. Therefore, a hydraulic conductivity on the firn within one order of magnitude to previous mountain glacier studies is a relatively small margin.

2.3 Crevasse Propagation

Crevasses are fractures in the ice that form from glacial movement and the resulting stress on the ice. These fractures open in the direction of maximum tension that is controlled by ice movement over the bed [*van der Veen,* 1998]. Since crevasses are proportional to local surface slope [*van der Veen,* 1998], changes in slope and ice thickness influence crevasse extent. Research shows that the extent of crevasses on the Greenland ice sheet has increased by 13% since the 1980s, likely due to the overall thinning and steepening of the ablation zone [*Colgan et al.,* 2011]. This is particularly concerning because, compared with a segment of ice not containing crevasses, the presence of crevasses doubles the solar radiation absorbed by the ice [*Pfeffer and Bretherton,* 1987]. As warming increases, crevasses will continue to provide a positive feedback mechanism enhancing glacial melt by reducing albedo and providing a means for water transport.

Crevasses are the most crucial avenues for water transport [*Fountain and Walder*, 1998], and research indicates that when crevasses are filled with water, crevasse propagation is increased by hydrofracture [*van der Veen,* 1998]. Glacial conduits will form from crevasses if the creep of ice closing the channel is exceeded or at least balanced by melt from flowing water [*Röthlisberger,* 1972]. Research indicates englacial conduits run throughout the glacier, as shown by video cameras lowered into boreholes, which revealed many englacial voids throughout the ice thickness [*Harper and Humphrey,* 1995]. Most frequently, conduits develop where flowing water is in contact with ice for the longest duration [*Röthlisberger,* 1972]. If the water supply is abundant, surface crevasses can penetrate to the glacier base causing increased glacial melt [*Benn et*

al., 2009]. It is suggested that water-filled crevasses are less likely to fracture in cold ice unless there is a sufficient source of water present, such as supraglacial lakes [*Alley et al.*, 2005]. The speed at which crevasses penetrate the ice depends on the fracture mechanics of the ice [*Weertman,* 1971]. This rate accelerates with increasing flow, but ice creep can block the flow of water from the crevasse [*Fountain and Walder,* 1998]. A steady water supply reduces the likelihood of creep pinching off the crevasse from its water source by keeping the conduit open to transport water to the base of the glacier.

2.4 Fracture Mechanics

Fracture mechanics is based on the assumption that all materials contain small cracks, which affect the integrity of a material. Stresses are higher near these defects, which can lead to enlargement, possibly to a point of fracture [*van der Veen,* 1998]. The fracture criterion for crevasses is debated as some researchers say that ice fractures as tensile stress reaches a critical value [*Vaughan,* 1993] while others say it depends on strain rates [*Vornberger and Whillans,* 1990]. Researchers also debate how depth crevasses penetrate the ice. In 1955, Nye assumed that a crevasse would propagate until the ice overburden pressure equals the tensile stress. Weertman [1973] questioned that Nye did not take into account stress concentrations near the crack tip and thus his model could only be applied to crevasse fields as opposed to individual isolated crevasses. Nye's method of estimating crevasse depth ignores the effect of stress concentrations existing in the immediate vicinity of the crevasse tip [*Weertman,* 1973]. This oversight is acceptable in a field of closely spaced crevasses due to the blunting effect where no tensile stress can exist and no large stress concentrations near the crevasse tip can develop. This effect promotes

downward propagation of neighboring crevasses on each other [*Weertman,* 1973]. Weetman's model takes into account both crevasse fields and isolated crevasses.

A significant source of water must be present to fracture crevasses. Lampkin et al. [2013] shows that supraglacial lakes ranging between 0.25-0.8 km in diameter, independent of volume, can fracture ice 1.5 km thick or less. This implies knowledge of surface hydrology which is critical for modeling crevasse propagation. The water supply for this study comes from the Greenland firn aquifer, which provides water to crevasses at varying depths, depending on the aquifer water table depth. By providing a steady supply of water, the aquifer may simulate repeated surface melt events. Multiple surface melt events allow for a more continuous surface water flow, which reduces resistance from the ice and allows cracks to fracture more readily [*Boon and Sharp*, 2003]. A water filled crevasse can penetrate to a mountain glacier or ice sheet bed, provided the water level is 15 m or less below the surface and the tensile stress is greater than approximately 150 kPa [*Vaughan,* 1993; *van der Veen,* 1998, *Boon and Sharp,* 2003]. Crevasse fracture is a positive feedback mechanism, meaning that once water proceeds to the glacier bed, ice flows more rapidly downstream from the crevasse. This widens the crevasse and allows more water to flow to the bed [*Boon and Sharp,* 2003]. Overall, crevasse propagation, once started, is likely to continue, allows more water to flow to the bed, and is enhanced by stresses which promote water flow into crevasses [*Alley et al.,* 2005].

The distribution of stresses near the crack tip can be quantified with the stress intensity factor. This factor is modeled as a function of the applied stress and has been calculated numerically and analytically according to geometry and applied stresses by various studies [*Sih,* 1973; *Tada et al.,* 1973]. The stress intensity factor is proportional to

crevasse depth, such that a greater depth means a larger stress intensity and a higher likelihood the crevasse will propagate the fracture to the bed of the ice sheet. It should be noted that stresses in firn are generally less than those in completely densified ice [*van der Veen,* 1998]. This is partially due to considerably smaller firn densities (~350 kg/m^3) than solid ice (~917 kg/m^3) [*Rist el al.,* 1996], which in turn reduces the stress intensity factors. The large variability of physical properties in firn make it difficult to quantify stresses required for failure [*Das et al.,* 2008].

This study will use three criteria, identified by Alley et al. [2005], to determine if crevasse propagation will occur. First, in order for propagation to occur, local tensile stress must be greater than the critical stress intensity. Secondly, as shown by van der Veen [1998] and Weertman [1973], the crack must remain filled with water because deviatoric stresses (stresses due to fluid motion) are not strong enough to counter hydrostatic stresses. Lastly, continued water flow into the crevasses is required so the water does not refreeze and block the crack. The crevasse deformation is assumed elastic in nature with crevasse surfaces free of traction. This culminates in an equation where, the sum of the stresses produced by hydrostatic pressure, tensile stress, and dislocations equal zero on all crevasse faces [*Weertman,* 1973], which maintains that forces and energy remain in equilibrium. Little study has been conducted on how water from the aquifer reaches the base of the glacier, so this study addresses glacial hydrology by studying crevasses as a means for water to proceed to the base of a glacier.

CHAPTER 3

DATA AND METHODS

This study utilizes a vertical profile of the subsurface aquifer from Operation Ice Bridge (OIB) radar data. The data uses ultra-high frequency radar, referred to as Accumulation Radar (AR), with a bandwidth of 300 MHz and a frequency of 750 MHz, thus enabling imaging of 65 cm vertical resolution [*Rodriquez-Morales et al.,* 2013]. National Aeronautics and Space Administration (NASA) Airborne Topographic Mapper (ATM) light detection and ranging (LIDAR) is used in parallel with AR radar to map surface elevation profiles along the AR transect. From individual OIB radar frames, a water table is defined when a continuous reflector is observed for at least 0.5 km horizontally. The AR detects the top of the aquifer because of a large dielectric contrast between the water filled firn and the dry firn above. However, the radar signal cannot penetrate through the aquifer due to increasing attenuation from the water, and thus cannot detect the lower bounds of the aquifer. From radar mapping of the top of the aquifer surface, the lateral flow within the aquifer can be investigated. These are the inputs used in Groundwater Modeling Systems (GMS) to estimate water flow volumes discharging from the aquifer into a crevasse. With the modeled discharge, conservation of mass and Weertman's [1973] equations of tensile stress are utilized to determine if enough water is available to propagate a fracture from the bottom of the preexisting

crevasse to the bed of the ice sheet. This study looks to explore englacial hydrology using the methods below, pictorially represented in Figure 1 to understand how melt water within the aquifer may exit the ice sheet, reach the ocean, contribute to sea level rise, and influence ice discharge from outlet glaciers by increasing ice speed.

3.1 Study Area

This research focuses on Helheim Glacier, shown in Figure 2, which is located in southeast Greenland along the lower elevation boundary of the Greenland firn aquifer. This location was chosen for ground-based measurements and airborne surveys because Helheim glacier is currently one of the fastest flowing outlets along the Greenland ice sheet and has experienced substantial thinning, leading to further glacial retreat [*Howat,* 2005]. Upon looking at WorldView imagery, the lateral extent of the aquifer coincides with a crevasse field, which also makes Helheim a desirable location. This research builds upon prior work that mapped the aquifer with airborne radar and ice surface topography with LIDAR remote sensing [*Miège et al.,* 2015].

Two field campaigns, along the Helheim transect, were conducted in April and August 2015. This study utilizes hydraulic conductivity data of the aquifer, water level fluctuations from pressure transducer measurements in a borehole within the aquifer, and air surface temperature measurements.

3.2 Aquifer Discharge

The discharge of water from the aquifer into a crevasse at its lower elevation termination is constrained by two independent estimates of water available to the crevasse. The analysis is conducted along an ice flow line feeding Helheim Glacier that runs perpendicular to the elevation contour lines and the crevasse orientation (Figure 2). The first method for estimating water availability to the crevasse uses a traditional terrestrial groundwater flow model and the second estimates the total surface melt that is produced along the profile. This profile is first modeled in SEEP2D [*Jones*, 1999], a 2D finite element groundwater model that is typically used to simulate groundwater flow within terrestrial aquifer systems by solving Darcy's law for every point along the depth profile. SEEP2D considers the aquifer to be a saturated, unconfined, steady state system and can be programmed to model complex groundwater flow. The SEEP2D flow cells depend on surface topography, and as water velocity increases, the flowlines become closer together. Flowlines are the same as streamlines in fluid mechanics literature, which are curves instantaneously tangent to the fluid velocity within the flow field [*Kundu and Cohen,* 2008]. The same amount of water discharges between each flowline, thus, if flowlines are closer together, velocity must correspondingly increase. This analysis assumes no flow into or out of the cross sectional plane and that Darcy's law is valid throughout the aquifer. SEEP2D assumes the modeled fluid is incompressible (valid for water) and simulated groundwater flow lines using Darcy's law (Equation 1). Darcy's law describes the flow of fluid through a porous media where Q is the volumetric flow rate (m^3/s), A the area (m^2), k the hydraulic conductivity (m/s), ΔL the change of length (m), and ΔH the head difference (m).

$$Q = kA\frac{\Delta H}{\Delta L} \quad (1)$$

The inputs needed for SEEP2D to estimate water discharge from the aquifer are therefore the variables described above in Darcy's law.

The SEEP2D inputs used to simulate the aquifer discharge along the Helheim transect are obtained from NASA airborne data and field measurements acquired by our team in April and August 2015. Two methods were used to measure hydraulic conductivity. The first was an "aquifer test" following the Theis [1935] method, in which two bore holes were drilled into the aquifer approximately one meter apart. Water was pumped out of one borehole which also caused the water level in the observational borehole to drop. The rate of water level recovery in the observational borehole was recorded with a pressure transducer attached to a data logger, every few seconds for about 75 min. The second method used to measure hydraulic conductivity was a "slug test," which involved displacing water within a single borehole and recording the time required for the water level to recover back to the level before displacement, following the Hvorslev [1951] method. Slug tests could be completed every few minutes, which is much quicker than the 75 min for an aquifer test. The slug tests are fast because they assess small aquifer water volumes, thus measuring the hydraulic conductivity over a smaller horizontal area of the aquifer. The mean hydraulic conductivity of the field site is 1.88×10^{-4} m/s, with a range of 8.8×10^{-5} m/s. This experimental hydraulic conductivity was one of two input parameters for SEEP2D. It should be noted that the hydraulic conductivity is not uniform through the entire transect, but due to field sampling limitations a single point wise

measurement of hydraulic conductivity was used.

The second input parameters were head fluctuations within the aquifer. As local flow cells within the aquifer are dependent on ice sheet surface topography, surface depressions act as discharge points for the aquifer, while areas of higher slope act as recharge points [*Miège et al.,* 2015]. Head values are equivalent to top of the aquifer water elevations along the profile. These are available approximately every 16 m along the transect from OIB radar and are assigned to each node in the SEEP2D simulation along the transect. At present time, there are no measurements of the variability of the basal boundary of the aquifer along a transect. Therefore, we use point measurements of aquifer thickness obtained from individual bores holes drilled through the aquifer. The model assumes a constant aquifer thickness of 25 m, which falls within the observational results found by Koenig et al. [2014], where the top of the aquifer was 12 m below the surface and extended to a depth of 37 m at pore close-off where there were no more interconnected pores between the ice grains. These parameters, modeled in SEEP2D, yield aquifer discharge into a crevasse at the lower elevation end of the transect which can then be used to determine if fracture propagation will occur within the crevasse. Here it is assumed that all the water from the firn will be routed to the crevasse system.

The discharge from SEEP2D generates an upper bound for aquifer discharge that can be compared with lower bound melt day measurements using a degree day melt model provided by Olivia Miller (manuscript in preparation, 2016). The degree day melt model is considered the lower bound because it represents the amount of possible melt for one season, while the SEEP2D is an upper bound since it represents a multiyear accumulation. A degree-day melt model assumes that, for each 1°C over 0°C, a certain

water equivalent of snow will be melted per day based on the daily average air temperature. The amount melted per day per degree over 0°C, is determined empirically for the region. This coefficient is then multiplied by the sum of the daily average temperatures above 0°C over the melt season [*Broeke et al.,* 2010]. The degree-day model provides the amount of snow melt recharge along the transect, which can then be multiplied by total area, to determine how much discharge is available to drain into the crevasse.

3.3 Pressure Required for Fracture Propagation within a Crevasse

With a constraint on aquifer discharge into a crevasse, the second part of this study works to identify whether the aquifer provides enough water discharge and corresponding pressure to propagate water to the ice sheet bed via hydrologic fracturing. Starting from basic principles of conservation of mass, the crevasse water depth, from the aquifer discharge, is calculated. Then, assuming various initial crevasse depths, tensile stress is calculated using Weertman's [1973] model. It can then be determined whether the resulting tensile stress is great enough to propagate a fracture within the crevasse to the base of the ice sheet using tensile strength values of glacial ice from the literature.

3.3.1 Fluid Mechanics Model

This model uses fluid mechanics, starting with the integral form of conservation of mass, to determine crevasse water depth based on discharge from the Greenland aquifer as modeled by SEEP2D or the melt day model. The equation for conservation of mass is shown below in Equation 2, where total mass equals the rate that mass accumulates

within the control volume, plus the rate of mass outflow across the control surface.

$$\frac{dM_{sys}}{dt} = \frac{\partial}{\partial t}\int_{cv}(\rho dV) + \int_{cs}(\rho\vec{v}\cdot d\vec{A}) = 0 \quad (2)$$

Here, ρ is the water density, $\vec{v}$ is velocity of water passing through the crevasse, V is water volume, and $\vec{A}$ is the cross sectional area at the inlet or outlet. Equation 2 reduces, as follows, to Equation 3 (complete simplification is found in the Appendix), assuming a unit length.

$$0 = \rho\frac{\partial}{\partial t}[A(h)] + \rho v_o A_o - \rho v_i A_i \quad (3)$$

H is the height of the water as a function of time, A is the area of the triangle with respect to height, A_0 and A_i are the cross sectional areas at the outlet and inlet, respectively. The crevasses are considered triangular, as shown below in Figure 3, to calculate the crevasse area solely as a function of height and angle at the crack tip. Figure 3 details how the dimensions of the triangle are defined for the derivation below in Equations 4, 5, and 6.

$$\tan(\theta) = \frac{b}{h} \quad (4)$$

$$b = h * \tan(\theta) \quad (5)$$

$$area = \frac{1}{2}bh = \frac{1}{2}h^2\tan(\theta) \quad (6)$$

The derivation in Equations 4, 5, and 6 detail how the triangle area is calculated. These

Equations (2-6) set up the foundation to calculate crevasse water depth.

Equation 3 then uses Equation 6 to model water depth for fracture when no water seeps out of the crevasse tip before failure occurs, yielding Equation 7. This means that water velocity exiting the crevasse is considered zero before fracture.

$$\frac{\partial}{\partial t}\left[\frac{1}{2}h(t)^2\tan(\theta)\right] = Q_i \tag{7}$$

This equation depends on Q_i, which is water flowing into the crevasse as discharge from the aquifer. Solving the differential equation by separation of variables yields the following solution for crevasse water depth in Equation 8.

$$h = \sqrt{\frac{2Q_i t}{\tan(\theta)}} \tag{8}$$

The complete derivation for calculating water height can be found in the Appendix. Tensile stress at the crevasse tip is then calculated from modeled water height in the crevasse.

3.3.2 Tensile Stress Calculation

The tensile stress for an isolated, water-filled crevasse is calculated using the method developed by Weertman in 1973. Following Weertman's method, the sum of the hydrostatic pressure (ρgy), tensile stress (T), and stress from dislocations ($\sigma_{xx}(y)$) must equal zero, as shown in Equation 9, where y is the glacial ice thickness measured from

the top surface.

$$-\rho g y + T + \sigma_{xx}(y) = 0 \tag{9}$$

This equation balances the forces at the crevasse tip. The stress from dislocations (anywhere atoms are out of alignment) is complex, and Kuang and Mura's [1968] answer for the general solution is utilized in this study. These equations assume that the crevasses are free of traction, thereby ignoring friction of water in the crevasse. Therefore, Equation 9 is coupled with Equation 10, where h is the water height, ρ' the density of water, and ρ the density of ice [*Weertman,* 1973].

$$-\rho g y - \rho' g(h - y) + T + \sigma_{xx}(y) = 0 \tag{10}$$

The general solution for Equation 9 and 10 is given by Weertman [1964]. The solution for tensile stress (T) and crevasse depth (L) is given in Equation 11.

$$L - \left(\frac{\pi T}{2\rho g}\right) + h\left(\frac{\rho'}{\rho}\right)\left[\frac{\pi}{2} - \sin^{-1}\left(\frac{h}{L}\right)\right] - \left(\frac{\rho'}{\rho}\right)(L^2 - h^2)^{\frac{1}{2}} = 0 \tag{11}$$

Equation 11 can be solved for tensile stress, shown in Equation 12, at various crevasse depths to determine if crevasse propagation will occur due to hydrofracture.

$$T = \frac{2\rho g}{\pi}\left[L + h\left(\frac{\rho'}{\rho}\right)\left[\frac{\pi}{2} - \sin^{-1}\left(\frac{h}{L}\right)\right] - \left(\frac{\rho'}{\rho}\right)(L^2 - h^2)^{\frac{1}{2}}\right] \tag{12}$$

Various crevasse geometries are modeled to build a framework and understand where fracture propagation within a crevasse is possible.

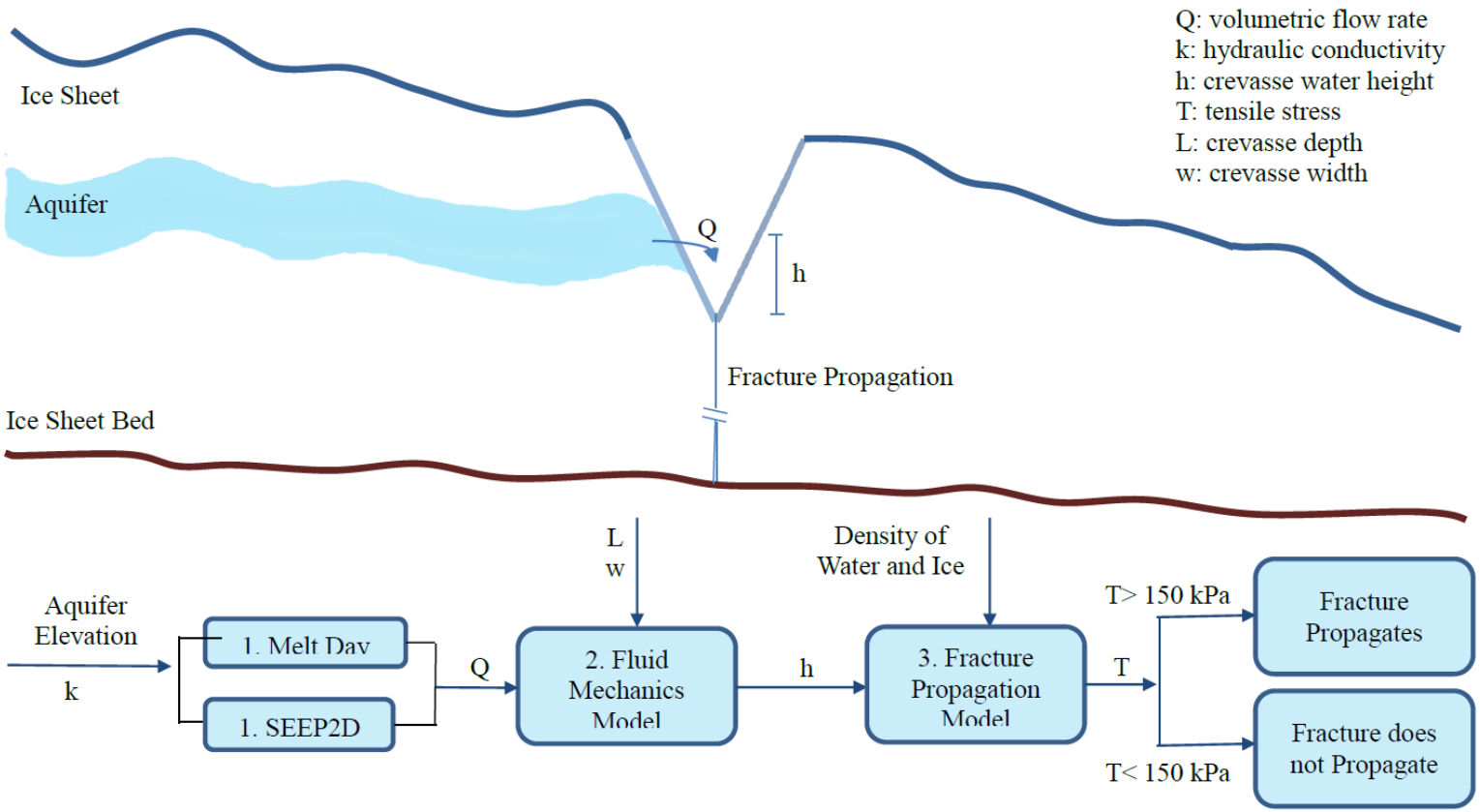

Figure 1: Schematic detailing model inputs and outputs. If the crevasse above has a high enough tensile stress, due to water from the aquifer, the fracture will propagate.

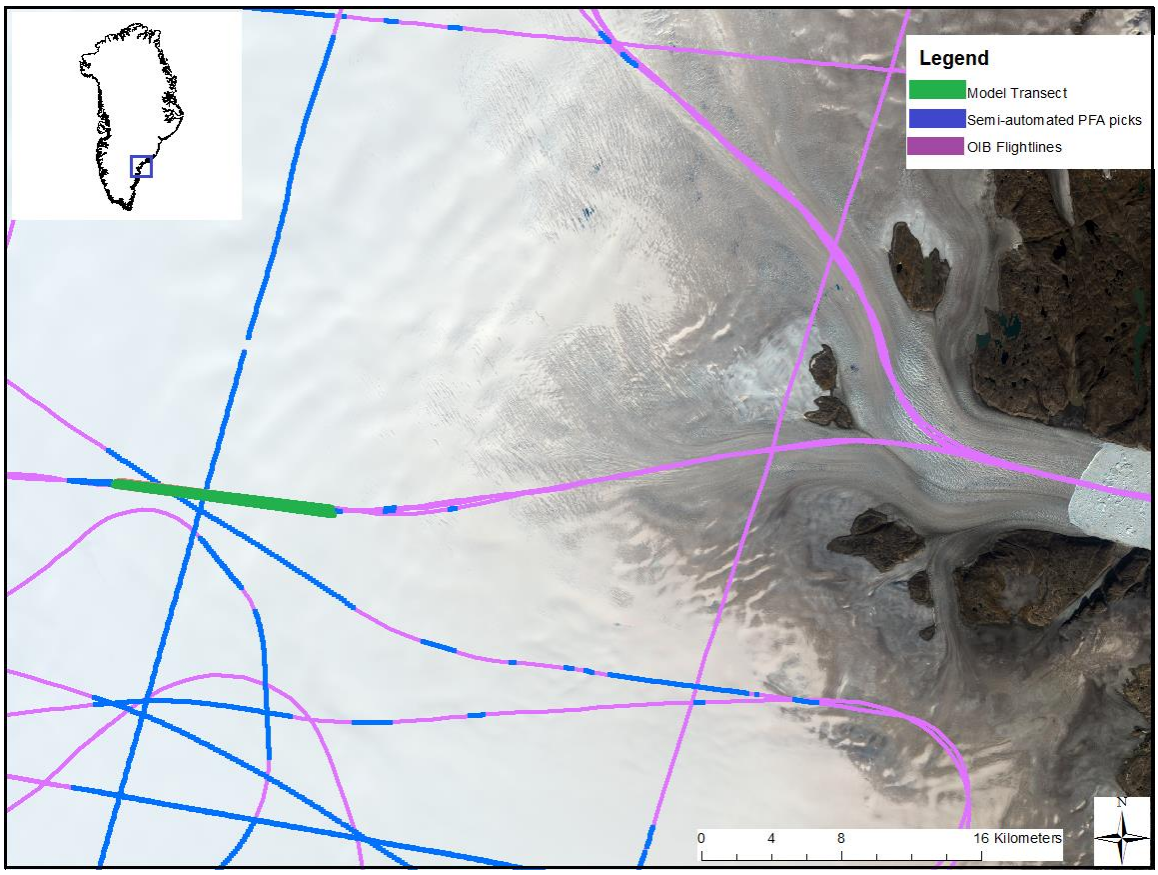

Figure 2: Image of Helheim Glacier and flight lines on the Greenland ice sheet. Locations of the perennial firn aquifer (PFA) are highlighted in blue, Operation Ice Bridge flightlines are outlined in purple, and the transect used in SEEP2D modeling is drawn in green using a Landsat 8 true color image acquired in August 2015.

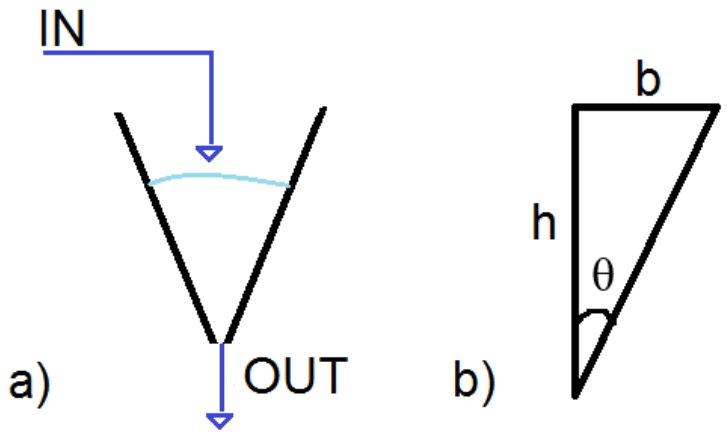

Figure 3: Crevasse dimensions for modeling water flow. (a) Water enters and exits a triangular crevasse (b) with corresponding modeling dimensions.

CHAPTER 4

RESULTS AND DISCUSSION

The results from both the aquifer discharge and crevasse fracture modeling are presented and discussed below. Field observations measured a hydraulic conductivity consistent with typical groundwater flow conditions. The SEEP2D and melt day modeling provide an upper and lower bound, respectively, for aquifer flow. It was found that, for several test cases, hydrofracture of an existing crevasse can occur. This means that certain crevasse geometries are capable of allowing water to propagate to the base of the ice sheet.

4.1 Aquifer Discharge

SEEP2D is utilized to model aquifer flow with inputs, boundary conditions, and assumptions, as described in the methods section. Assuming no water flows into or out of the cross section and that Darcy's law is valid, SEEP2D simulates an average total flow rate of 15,260 m^3/yr per meter width of the profile. These results were conducted with a hydraulic conductivity value of 1.88×10^{-4} m/s that was measured on the Greenland ice sheet by the field team in April 2015. As seen in Figure 4, flow cells are highly correlated to surface topography. Head values are assigned to each node along the top of the transect, which means that head fluctuations translate to drainage rates.

The area between two adjacent flowlines is known as a flowtube. The discharge through each flowtube is uniform. This means that velocity increases when the width between flowtubes is smaller, and decreases when that width is greater. Helheim Glacier discharge results and the modeled flowlines through the aquifer are plotted against elevation and distance along the transect (Figure 4). Discharge locations may be manifested as thick subsurface ice layers, where water moving vertically upwards is refrozen as it moves into colder firn. Based on the model results, all of the flow appears to be coming from one kilometer previously along the transect. Therefore, the total flow used in the modeling only includes the discharge from the last kilometer of the transect. However, the assumption of homogeneous hydraulic conductivity with depth implies that the flow paths would be different from a real heterogeneous system, since water flows more slowly through regions of low hydraulic conductivity, and more quickly through regions of high hydraulic conductivity. For example, Miège et al. has determined that there is evidence of thick ice layers (very low hydraulic conductivity) within the firn that may be evidence of a mechanism for discharge along the transect (manuscript in preparation, 2015).

The flow was calculated with an assumed 25 m thick aquifer, which agrees with measured results [*Koenig et al.,* 2014]. However, the aquifer thickness may change along the transect as hydraulic gradients vary spatially. Since radar signals cannot penetrate to the lower margins of the aquifer, due to signal attenuation from the water and limited field sampling, a constant 25 m aquifer thickness is the currently accepted value. This offers room for future study if more detailed field measurements can be obtained. Flow is likely altered due to the presence of ice lenses which hinders vertical water flow and

therefore changes horizontal water movement. Even though densification competes with the slow lateral flow through the aquifer via compaction [*Koenig et al.,* 2014], the lateral flow persists. Figure 4 also implies that water may be entering and exiting the aquifer along the transect.

The SEEP2D results were compared with the degree-day melt model. The degree-day melt model yields an available recharge based on season melt of 0.5 m/yr. For one meter width along the entire transect, this means a 6,000 m^3/yr of possible recharge. This value is about half the discharge simulated with SEEP2D (15,260 m^3/yr per m of transect). Further constraints must be found to better quantify discharge into crevasses, but combining SEEP2D analysis with the recharge model does provide an initial set of constraints for discharge into a crevasse.

4.2 Tensile Stress Required for Fracture

From the calculated water flow using the SEEP2D (Figure 5) output and recharge measurements (Figure 6), tensile stress is calculated for an array of crevasse dimensions. In these figures, the values to the left of the black diagonal line-segments do not propagate fracture in the crevasse, but values at the black diagonal line-segments or right of them do yield fracture. This provides insight into what parameters must be met in order for crevasses receiving water from the aquifer to fracture to the base of the ice sheet. For deep crevasses with small widths, fracture can occur in a matter of weeks. Twenty-five crevasse widths were measured using August 2015 WordView 1 imagery from DigitalGlobe© (Figure 7), which shows the width of crevasses to be 8.5 m on average with a standard deviation of 3 m. The largest crevasse width measured was 14 m,

and considering image resolution of ±1 m, an upper width bound of 15 m was used. These widths were measured on Helheim Glacier near the end of the modeled transect within close proximity to the field sites. The fracture propagation analysis indicates that an average width of 8.5 m falls within the range of possible fracture propagation. It is hypothesized that more focused stresses exist at the crevasse tip of thin crevasses compared with wider water-filled fractures, thus enabling fracture propagation to occur more readily for small crevasse widths, like those measured on Helheim.

Fracture propagation occurs much more quickly using SEEP2D simulated aquifer discharge into a crevasse compared to the melt day modeled discharge. Within one standard deviation of crevasse widths, crevasse fracture for the SEEP2D simulation can occur after 30 days of being filled from the aquifer, if the crevasse is 30 m deep, or after 21 days, if the crevasse is 35 m deep. One crevasse, out of 25, was observed to have a width of 3 m, which indicates the possibility of fracture propagation for a 30 m deep crevasse after 37 days for the recharge model. With an initial crevasse depth of 35 m, the recharge model predicts that fracture propagation at widths within one standard deviation of the mean can occur after 33 days.

Fracture propagation does still occur for both methods of discharge estimation but the melt day model results indicate that fewer crevasse geometries will allow propagation. These models assume constant water flow from the aquifer, which is likely true for some weeks in the summer but not during the winter when it is likely that, while water still flows within the aquifer, it would probably freeze upon entering a crevasse. Based on an air temperature time series at the field site in 2015, there are approximately 50 days with average temperatures above 0°C. Therefore, if fracture propagation does not occur within

a 50 day melt window, it is assumed that propagation will not occur. It is also assumed that, during the summer, crevasses are open to the atmosphere and not filled with snow. In the winter, an ice plug may form as the aquifer water freezes upon contact with frigid atmospheric air. Winter water movement is still a question requiring further study. For both SEEP2D and melt day calculations, threshold for fracture exists more extensively with crevasse depths greater than 30 m. For the following analysis, a crevasse depth of 30 m is used with SEEP2D.

It should be noted that hydraulic conductivity plays a large role in determining the feasibility of crevasse propagation. Hydraulic conductivity is directly proportional to water flow, due to the relationship with Darcy's Law. Therefore, even subtle changes in hydraulic conductivity can vastly affect the flow values. The average field value measured near the Helheim site (1.88×10^{-4} m/s) is used primarily, but the error bounds of this measurement yield large variations on the flow calculations. In order to assess the sensitivity of the uncertainty, the results for two additional hydraulic conductivity values are displayed, in Figure 8, for a 30 m deep crevasse. Although the hydraulic conductivity has a large impact on the time duration until fracture propagation, the three cases shown in Figure 8 all yield fracture within the time scale of one summer season. Even with hydraulic conductivities varying within the measurement range, crevasses are likely to propagate aquifer water to the ice sheet bed. This hydrofracture process is a positive feedback mechanism, because once a fracture exists, water can continuously propagate to the bed and widen the fracture as more water carves out the sides of the fractured vertical conduit. Water filled crevasses also have the positive feedback mechanism of decreasing the albedo, increasing absorption of the sun's energy into the ice sheet and hence

widening the crevasse [*Stocker,* 2014]. This enhances ice sheet melt and increases water output into the ocean. These results imply that crevasses offer a possible outlet to the ocean, allowing the firn aquifer to directly contribute to sea level rise and increased glacial flow velocity.

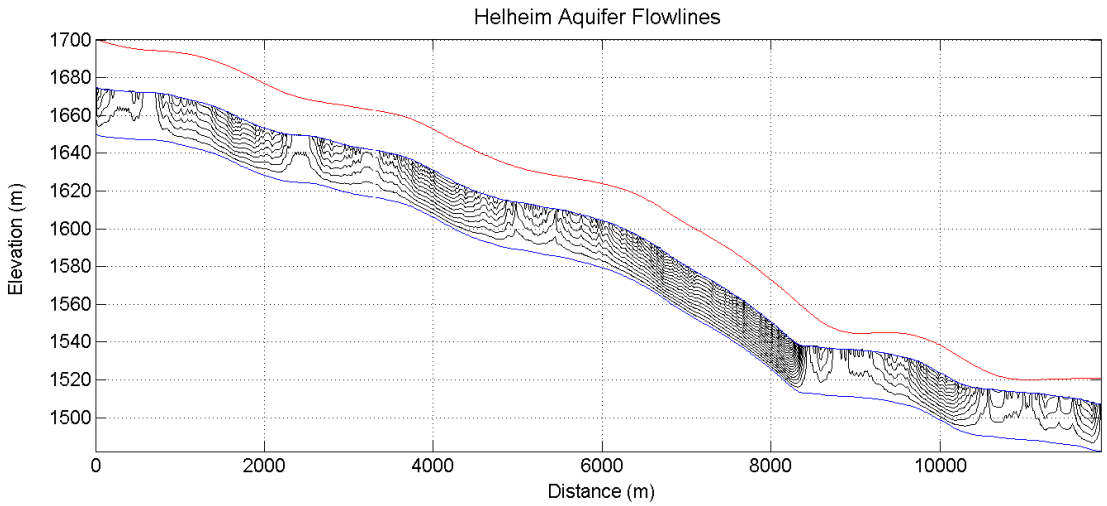

Figure 4: Helheim flowlines through the Greenland aquifer. The red line shows the ice sheet surface, blue lines outline the extent of the aquifer, and black lines represent water flow through the aquifer. A preexisting crevasse is assumed to be located at the lower elevation termination of the aquifer.

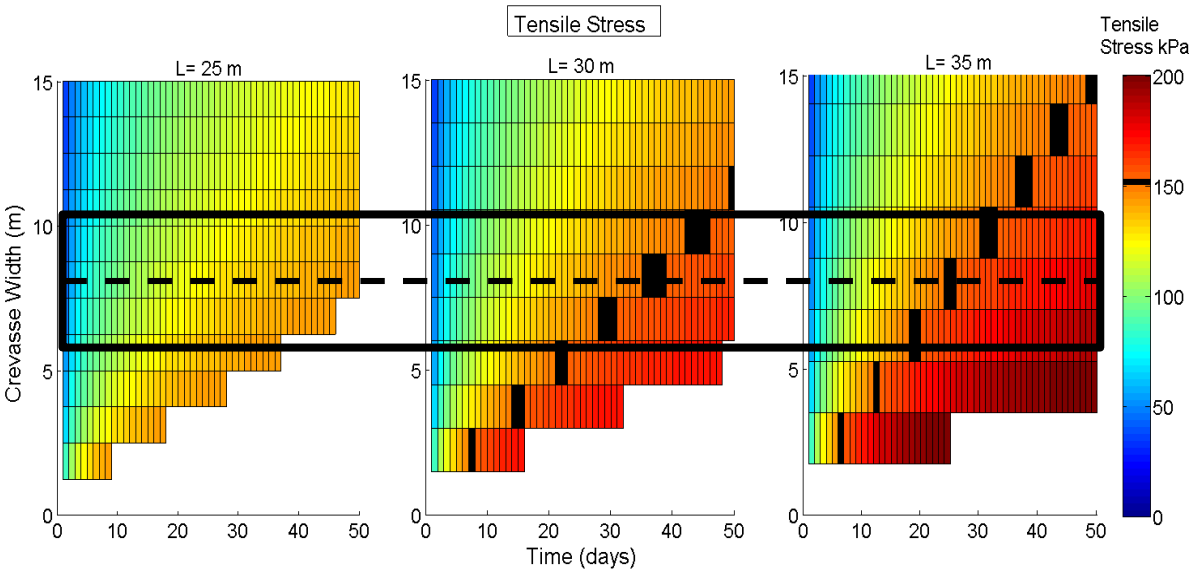

Figure 5: Tensile stress for crevasses using SEEP2D discharge results. Crevasse depth (L) is modeled at 25, 30, and 35 m with varying widths over a time period of 50 days. The dashed line is mean crevasse widths measured on Helheim while the boxed area indicates one standard deviation around these average widths. The black diagonal line-segments are the 150 kPa tensile stress criteria used for ice fracture.

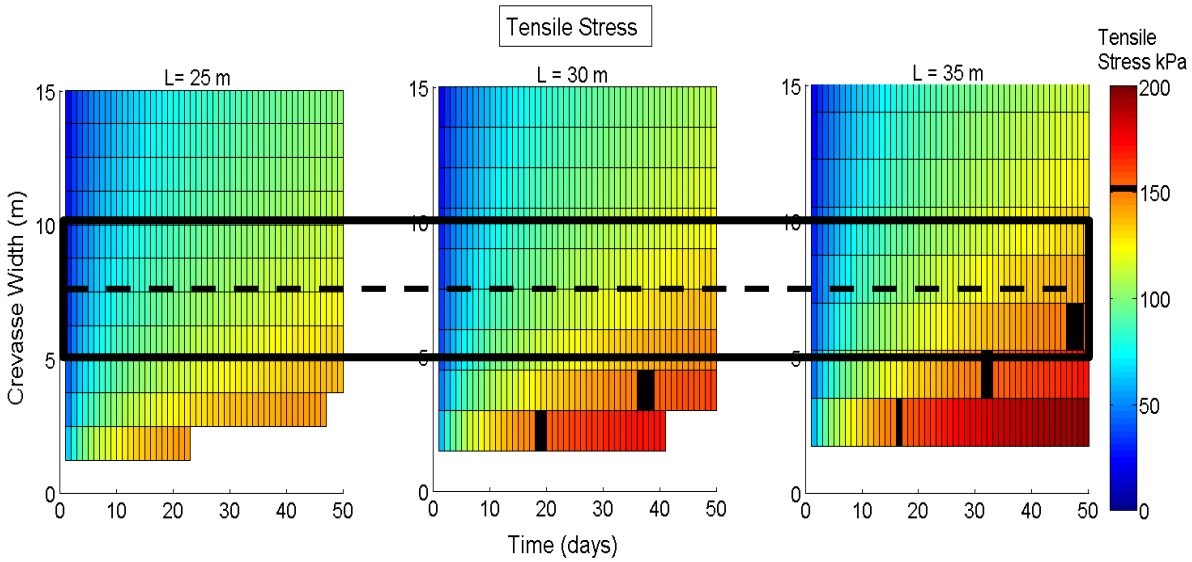

Figure 6: Tensile stress for crevasses using melt day results. Crevasse depth (L) is modeled at 25, 30, and 35 m with varying widths over a time period of 50 days. The dashed line is mean crevasse widths measured on Helheim while the boxed area indicates one standard deviation around these average widths. The black diagonal line-segments are the 150 kPa tensile stress criteria used for ice fracture.

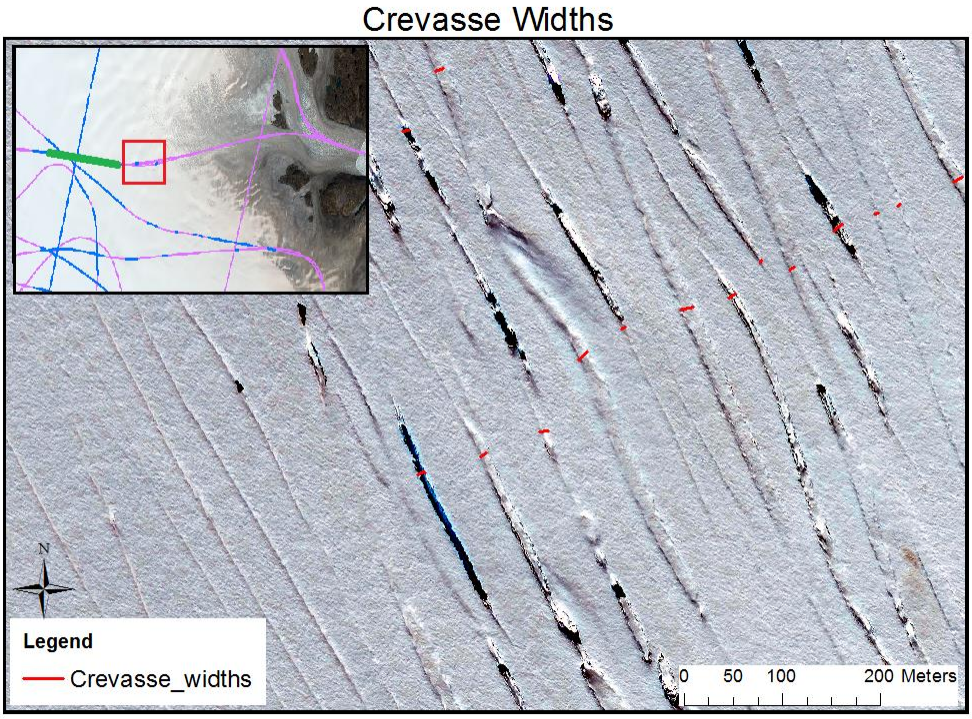

Figure 7: Crevasse width measurements on Helheim glacier. Worldview 1 August 2015 true color imagery from DigitalGlobe© is used to measure the widths (15 of the 25 measurements are displayed in this image). The location of the crevasses with respect to Helheim glacier is shown in the upper left corner.

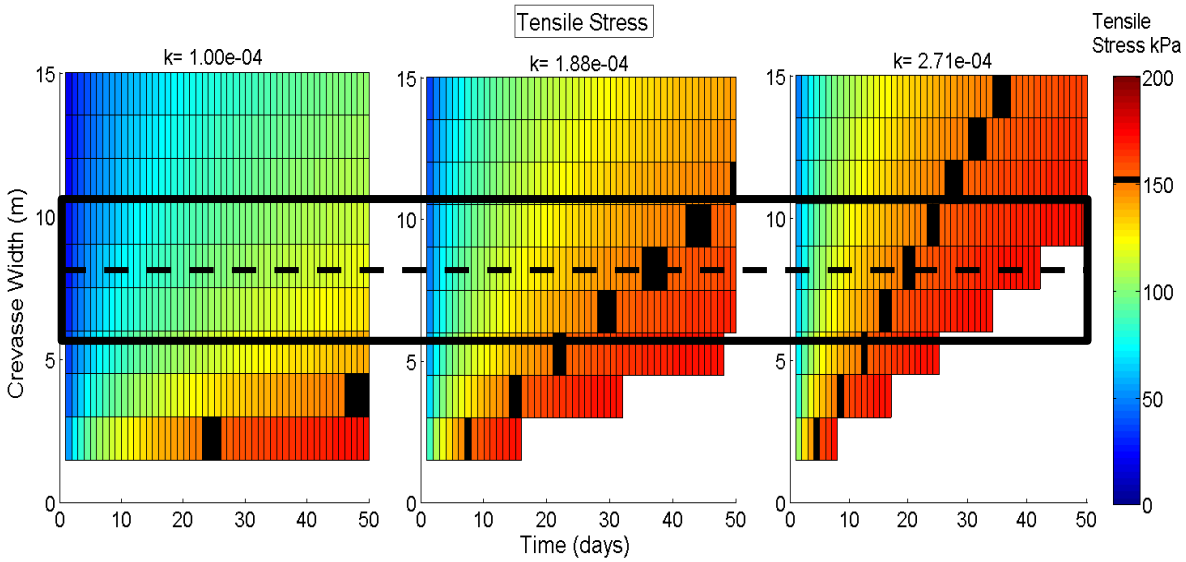

Figure 8: Tensile stress plots for 30 m deep crevasses at varying hydraulic conductivities (k). The dashed line is mean crevasse widths measured on Helheim while the boxed area indicates one standard deviation around these average widths. The k values shown represent the mean, upper, and lower ranges of sampled k. The black diagonal line-segments are the 150 kPa tensile stress criteria used for ice fracture.

CHAPTER 5

CONCLUSION

This research provides an initial analysis to examine a mechanism that allows water in the Greenland firn aquifer to exit the ice sheet via crevasses. These results indicate hydraulic fracturing of crevasses is possible, meaning that the aquifer has an outlet mechanism to release water into the ocean, therefore contributing to sea level rise. SEEP2D discharge quantification represents an upper bound of water flow into a terminal crevasse yielding 15,260 m^3/yr per meter width of the transect while melt day calculations yield a lower bound of 6,000 m^3/yr per meter width. For crevasses 30 m or greater in depth, fracture propagation is possible within a summer season after 30 days according to SEEP2D modeling and after 37 days for the melt day modeling. However, some assumptions have been made. For example, water flow through the ice is considered uniform in order to solve conservation of mass. The flow is known to be turbulent, but uniform assumptions allow a close-formed solution. A uniform assumption is made in all groundwater modeling applications making this a viable first-order assumption for flow within the Greenland aquifer. In the SEEP2D model, the flow is considered to be one-dimensional. This means that crevasses extend infinitely in the transverse direction, which is a reasonable estimate as a starting basis (Figure 7). Another assumption is that crevasses will propagate a fracture when critical conditions of

stress are exceeded on the ice surface [*Kehle,* 1964; *Vaughan,* 1993], which is a fully accepted condition in the glaciology literature. It is also assumed that there is a constant discharge and that tensile stress, density, temperature, and hydraulic conductivity are constant throughout the ice thickness. Difficulty of field sampling and limited resources constrain this as the only currently feasible option. These assumptions are within the reasonable realm for an initial analysis to understand crevasses as a possible outlet mechanism for water in the Greenland firn aquifer to reach the ocean.

APPENDIX

HYDRAULIC FRACTURE DERIVATION

Below is the full derivation for the hydraulic fracturing model. This derivation starts with conservation of mass in Equation 2 and ends with an equation for water fill height.

$$\frac{dM_{sys}}{dt} = \frac{\partial}{\partial t}\int_{cv}(\rho dV) + \int_{cs}(\rho\vec{v}\cdot d\vec{A}) = 0 \tag{13}$$

$$0 = \rho\frac{\partial}{\partial t}[A(h)] + \rho v_o A_o - \rho v_i A_i \tag{14}$$

$$\frac{\partial}{\partial t}\left[\frac{1}{2}h(t)^2\tan(\theta)\right] = Q_i - v_2 A_o \tag{15}$$

$$\frac{\partial}{\partial t}\left[\frac{1}{2}h(t)^2\tan(\theta)\right] = Q_i - 0 \tag{16}$$

$$h(t)\tan(\theta)\frac{\partial h(t)}{\partial t} = Q_i \tag{17}$$

$$\tan(\theta)\int h(t)\partial h(t) = Q_i\int \partial t \tag{18}$$

$$\frac{1}{2}\tan(\theta)h(t)^2 = Qt \tag{19}$$

$$h = \sqrt{\frac{2Q_i t}{\tan(\theta)}} \tag{20}$$

REFERENCES

Alley, R. B., T. K. Dupont, B. R. Parizek, and S. Anandakrishnan (2005), Access of surface meltwater to beds of sub-freezing glaciers: Preliminary insights, A*nn. Glaciol.*, *40*, 8-14.

Bamber, J., J. Griggs, R. Hurkmans, J. Dowdeswell, S. Gogineni, I. Howat, J. Mouginot, J. Paden, S. Palmer, and E. Rignot (2013), A new bed elevation dataset for Greenland, *The Cryosphere*, *7*(2), 499-510.

Benn, D., J. Gulley, A. Luckman, A. Adamek, and P. S. Glowacki (2009), Englacial drainage systems formed by hydrologically driven crevasse propagation, *J. Glaciol.*, *55*(191), 513-523.

Boon, S., and M. Sharp (2003), The role of hydrologically-driven ice fracture in drainage system evolution on an Arctic glacier, *Geophys. Res. Lett.*, *30*(18).

Braun, L., M. Weber, and M. Schulz (2000), Consequences of climate change for runoff from Alpine regions, *Ann. Glaciol.*, *31*(1), 19-25.

Catania, G. A. (2008), Characterizing englacial drainage in the ablation zone of the Greenland ice sheet. *J. Glaciol.*, 54(187), 567-578.

Chu, V. W. (2014), Greenland ice sheet hydrology: A review, *Progr. Phys. Geogr.*, *38*(1), 19-54.

Colgan, W., K. Steffen, W. S. McLamb, W. Abdalati, H. Rajaram, R. Motyka, T. Phillips, and R. Anderson (2011), An increase in crevasse extent, West Greenland: Hydrologic implications, *Geophys. Res. Lett.*, *38*(18).

Cuffey, K. M., and W. S. B. Paterson (2010), *The physics of glaciers*, Academic Press, Massachusetts.

Das, S. B., I. Joughin, M. D. Behn, I. M. Howat, M. A. King, D. Lizarralde, and M. P. Bhatia (2008), Fracture propagation to the base of the Greenland ice sheet during supraglacial lake drainage, *Science*, *320*(5877), 778-781

De Woul, M., R. Hock, M. Braun, T. Thorsteinsson, T. Jóhannesson, and S.

Halldorsdottir (2006), Firn layer impact on glacial runoff: a case study at Hofsjökull, Iceland, *Hydrol. Processes*, *20*(10), 2171-2185.

Doyle, S. H., A. Hubbard, C. F. Dow, G. A. Jones, A. Fitzpatrick, A. Gusmeroli, B. Kulessa, K. Lindback, R. Pettersson, and J. E. Box (2013), Ice tectonic deformation during the rapid in situ drainage of a supraglacial lake on the Greenland Ice Sheet, *The Cryosphere*, *7*(1), 129-140.

Forster, R. R., J. Box, M. van den Broeke, C. Miège, E. Burgess, J. van Angelen, J. Lenaerts, L. Koenig, J. Paden, C. Lewis, S. Gogineni, C. Leuschen, J. McConnell (2014), Extensive liquid meltwater storage in firn within the Greenland ice sheet, *Nature Geosci.*, *7*(2), 95-98.

Fountain, A. G. (1989), The storage of water in, and hydraulic characteristics of, the firn of South Cascade Glacier, Washington State U.S.A. *Ann. of Glaciol.*, 13, 69-75.

Fountain, A. G., and J. S. Walder (1998), Water flow through temperate glaciers, *Rev. Geophys.*, *36*(3), 299-328.

Hanna, E., P. Huybrechts, K. Steffen, J. Cappelen, R. Huff, C. Shuman, T. Irvine-Fynn, S. Wise, and M. Griffiths (2008), Increased runoff from melt from the Greenland Ice Sheet: a response to global warming, *J. Climate*, *21*(2), 331-341.

Harper, J. T., and N. F. Humphrey (1995), Borehole video analysis of a temperate glacier englacial and subglacial structure: Implications for glacier flow models, *Geology*, *23*(10), 901-904.

Harper, J., N. Humphrey, W. T. Pfeffer, J. Brown, and X. Fettweis (2012), Greenland ice-sheet contribution to sea-level rise buffered by meltwater storage in firn, *Nature*, *491*(7423), 240-243.

Howat, I. M., I. Joughin, S. Tulaczyk, and S. Gogineni (2005), Rapid retreat and acceleration of Helheim Glacier, east Greenland, *Geophys. Res. Lett.*, *32*(22).

Hvorslev, M. J. (1951), Time lag and soil permeability in ground-water observations, Report to the Waterways Experiment Station, Corps of Engineers, 1-55.

Jansson, P. (1995), Water pressure and basal sliding on Storglaciären, northern Sweden, *J. Glaciol.*, *41*(138), 232-240.

Jansson, P., R. Hock, and T. Schneider (2003), The concept of glacier storage: a review, *J. Hydrol.*, *282*(1), 116-129.

Jones, N. L. (1999), *SEEP2D Primer*, Environmental Modeling Research Laboratory, Brigham Young University.

Kawashima, K., T. Yamada, and G. Wakahama (1993), Investigations of internal structure and transformational processes from firn to ice in a perennial snow patch, *Ann. Glaciol*, *18*, 117-122.

Kehle, R.O. (1964), Deformation of the Ross Ice Shelf, Antarctica. *Geophys. Soc. Am. Bull.*, 75, 259-286.

Koenig, L. S., C. Miège, R. R. Forster, and L. Brucker (2014), Initial *in situ* measurements of perennial meltwater storage in the Greenland firn aquifer, *Geophys. Res. Lett.*, *41*(1), 81-85.

Kuang, J. G., and T. Mura (1968), Dislocations pile-up in two-phase materials, *J. Appl. Phys.*, 39(1), 109-120.

Kundu, P. K., I. Cohen, D. Dowling (2012), *Fluid Mechanics*, 5th ed. Academic Press, Waltham.

Lampkin, D., N. Amador, B. Parizek, K. Farness, and K. Jezek (2013), Drainage from water-filled crevasses along the margins of Jakobshavn Isbræ: A potential catalyst for catchment expansion, *J. Geophys. Res.*, *118*(2), 795-813.

Miège, C., R. R. Forster, J. E. Box, E. W. Burgess, J. R. McConnell, D. R. Pasteris, and V. B. Spikes (2013), Southeast Greenland high accumulation rates derived from firn cores and ground-penetrating radar, *Ann. Glaciol.*, *54*(63), 322-332.

Miège C., R. Forster, L. Brucker, L. Koenig, D. Solomon, J. Paden, J. Box, E. Burgess, J. Miller, L. McNerney, N. Brautigam, R. Fausto, S. Gogineni, (2015), Spatial extent and temporal variability of the Greenland firn aquifer detected by ground and airborne radars, (In Review).

Munneke, P. K., S. M Ligtenberg, M. Broeke, J. Angelen, and R. Forster (2014), Explaining the presence of perennial liquid water bodies in the firn of the Greenland Ice Sheet, *Geophys. Res. Lett.*, *41*(2), 476-483.

Nye, J.F., (1955). Comments of Dr. Loewe's letter and notes on crevasses. *J. Glaciol.,* 2, 512-514.

Oerter, H., and H. Moser (1982), Water storage and drainage within the firn of a temperate glacier (Vernagtferner, Oetztal Alps, Austria), *Hydrological Aspects of Alpine and High-Mountain Areas Symposium,* 71-81.

Pfeffer, W. T., and C. S. Bretherton (1987), The effect of crevasses on the solar heating of a glacier surface, *IAHS Publ.*, *170*, 191-205

Pfeffer, W. T., M. F. Meier, and T. H. Illangasekare (1991), Retention of Greenland runoff by refreezing: implications for projected future sea level change, *J.*

Geophys. Res., 96(C12), 22117-22124.

Rennermalm, A., S. Moustafa, J. Mioduszewski, V. Chu, R. Forster, B. Hagedorn, J. Harper, T. Mote, D. Robinson, and C. Shuman (2013), Understanding Greenland ice sheet hydrology using an integrated multi-scale approach, *Environ. Res. Lett.*, *8*(1), 015017.

Rist, M., P. Sammonds, S. Murrell, P. Meredith, H. Oerter, and C. Doake (1996), Experimental fracture and mechanical properties of Antarctic ice preliminary results, *Ann. Glaciol.*, *23*, 284-292.

Rodriguez-Morales, F., S. Gogineni, C. J. Leuschen, J. D. Paden, J. Li, C. C. Lewis, B. Panzer, D. Gomez-Garcia Alvestegui, A. Patel, and K. Byers (2014), Advanced multifrequency radar instrumentation for polar research, *Geosci. Remote Sens.*, *52*(5), 2824-2842.

Röthlisberger, H. (1972). Water pressure in intra- and subglacial channels. *J. Glaciol.*, 11, 177-203.

Sasgen, I., M. van den Broeke, J. L. Bamber, E. Rignot, L. S. Sørensen, B. Wouters, Z. Martinec, I. Velicogna, and S. B. Simonsen (2012), Timing and origin of recent regional ice-mass loss in Greenland, *Earth Planet. Sci. Lett.*, *333*, 293-303.

Schneider, T. (1999), Water movement in the firn of Storglaciaren, Sweden, *J. Glaciol.*, *45*(150), 286-294.

Schwartz, F. W., and H. Zhang (2003), *Fundamentals of ground water*, Wiley New York.

Shepherd, A., E. R. Ivins, A. Geruo, V. R. Barletta, M. J. Bentley, S. Bettadpur, K. H. Briggs, D. H. Bromwich, R. Forsberg, and N. Galin (2012), A reconciled estimate of ice-sheet mass balance, *Science*, *338*(6111), 1183-1189.

Sih, G.C., (1973), Handbook of Stress Intensity Factors. Institute of Fracture and Solid Mechanics, Le High University, Bethlehem, PA.

Stocker, T., D. Qin, G.-K. Plattner, M. Tignor, S. K. Allen, J. Boschung, A. Nauels, Y. Xia, V. Bex, and P. M. Midgley (2014), *Climate change 2013: The physical science basis*, Cambridge Univ. Press Cambridge, UK, and New York.

Tada, H., Paris, P.C., Irwin, G.R., (1973), The Stress Analysis of Cracks Handbook. Del Research Corporation, Hellertown, PA.

Tedesco, M., and N. Steiner (2011), In-situ multispectral and bathymetric measurements over a supraglacial lake in western Greenland using a remotely controlled

watercraft, *The Cryosphere*, *5*(2), 445-452.

Tedesco, M., I. C. Willis, M. J. Hoffman, A. F. Banwell, P. Alexander, and N. S. Arnold (2013), Ice dynamic response to two modes of surface lake drainage on the Greenland ice sheet, *Environ. Res. Lett.*, *8*(3).

Theis, C. V. (1935), *The relation between the lowering of the piezometric surface and the rate and duration of discharge of a well using ground water storage*, US Department of the Interior, Geological Survey, Water Resources Division, Ground Water Branch Washington, DC.

van de Wal, R., W. Boot, M. van den Broeke,C. Smeets, C. Reijmer, J. Donker, and J. Oerlemans (2008), Large and rapid melt-induced velocity changes in the ablation zone of the Greenland ice sheet, *Science*, *321*(5885), 111-113.

van den Broeke, M., J. Bamber, J. Ettema, E. Rignot, E. Schrama, W. J. D. van Berg, E. van Meijgaard, I. Velicogna, and B. Wouters (2009), Partitioning recent Greenland mass loss, *Science*, *326*(5955), 984-986.

van den Broeke, M., C. Bus, J. Ettema, and P. Smeets (2010), Temperature thresholds for degree-day modelling of Greenland ice sheet melt rates, *Geophys. Res. Lett.*, *37*(18).

van der Veen, C. (1998), Fracture mechanics approach to penetration of surface crevasses on glaciers, *Cold Regions Sci. Technol.*, *27*(1), 31-47.

Vaughan, D. G. (1993), Relating the occurrence of crevasses to surface strain rates, *J. Glaciol.*, *39*(132), 255-266.

Vornberger, P., and I. Whillans (1990), Crevasse deformation and examples from Ice Stream B, Antarctica, *J. Glaciol.*, *36*(122), 3-10.

Walder, J. S. (2010), Röthlisberger channel theory: its origins and consequences, *J. Glaciol., 56*(200), 1079-1086.

Weertman, J. (1971), Velocity at which liquid-filled cracks move in the Earth's crust or in glaciers, *J. Geophys. Res.*, *76*(35), 8544-8553.

Weertman, J. (1973), Can a water-filled crevasse reach the bottom surface of a glacier, *IASH Publication*, *95*, 139-145.

Weertman (1964), Continuum distribution of dislocations on faults with finite friction. *Bull. Seismol. Soc. Am.*, 54(4), 1035-1058.

Zwally, H. J., W. Abdalati, T. Herring, K. Larson, J. Saba, and K. Steffen (2002),

Surface melt-induced acceleration of Greenland ice-sheet flow, *Science*, *297*(5579), 218-222.

Zwally, H. J., L. Jun, A. C. Brenner, M. Beckley, H. G. Cornejo, J. Dimarzio, M. B. Giovinetto, T. A. Neumann, J. Robbins, and J. L. Saba (2011), Greenland ice sheet mass balance: Distribution of increased mass loss with climate warming; 2003–2007 versus 1992–2002, *J. Glaciol.*, *57*(201), 88-102.